Carbohydrate Polymers 88 (2012) 1093–1099

Contents lists available at SciVerse ScienceDirect

Carbohydrate Polymers

journal homepage: www.elsevier.com/locate/carbpol

Reinforced low density alginate-based aerogels: Preparation, hydrophobic modification and characterization

Yi Cheng, Lingbin Lu*, Wuyuan Zhang, Jianjun Shi, Yang Cao

Key Laboratory of Ministry of Education for Application Technology of Chemical Materials in Hainan Superior Resources, School of Materials and Chemical Engineering, Hainan University, Haikou, 570228 Hainan, China

ARTICLE INFO

Article history:
Received 8 December 2011
Received in revised form 12 January 2012
Accepted 23 January 2012
Available online 30 January 2012

Keywords:
Alginate aerogel
Biodegradable
Cold plasma
Hydrophobic modification
Reinforcement

ABSTRACT

Homogeneous reinforced low density alginate-based aerogel was prepared by ionotropic gelation of sodium alginate. N,N′-methylenebisacrylamide and carboxy-methylcellulose were introduced into the alginate hydrogel matrix as reinforcing agents, respectively. Analysis of FTIR spectra showed that the reinforcing agents had strong interaction with alginate through hydrogen bond, which enhanced the aerogel's compression strength effectively. Meanwhile, density and volume shrinkage of the aerogels retained at an appropriate low level. Highly hydrophobic aerogels were obtained by the following targeted modification using a CCl_4 plasma treatment. Together with hydrophobicity, the alginate-based aerogels can be used as potential biodegradable, lightweight and oil-absorptive materials.

1. Introduction

Natural polymers with biodegradability, biocompatibility, natural abundance and unique physicochemical/biological properties are of great interest during recent years (Augst, Kong, & Mooney, 2006; Božanić, Trandafilović, Luyt, & Djoković, 2010; Chan, Whitney, & Neufeld, 2009; Dang & Leong, 2006; Quignard, Valentin, & Di Renzo, 2008). Alginate, one of the most abundant natural polysaccharides, is extracted from brown algae and has a number of merits such as nontoxicity, biocompatibility, hydrophilicity, nonimmunogenicity, etc. (Shapiro & Cohen, 1997). Hence, alginate is extensively investigated in foods, pharmaceuticals, regenerative medicine and chemical engineering (Chung et al., 2002; Dar, Shachar, Leor, & Cohen, 2002; Draget, Smidsrød, & Skjåk-Bræk, 2002; Hashimoto, Suzuki, Tanihara, Kakimaru, & Suzuki, 2004; Mierisch et al., 2002). The most valuable and potential studies are alginate-based hydrogels and aerogels (Donati et al., 2005; Robitzer, David, Rochas, Di Renzo, & Quignard, 2008; Robitzer, Di Renzo, & Quignard, 2011; Wang et al., 2011). Owing to the biocompatibility and simple gelation with divalent cations such as Ca^{2+}, alginate is widely used for cell immobilization and encapsulation. Alginate hydrogels are formed when divalent or trivalent cations coordinate to the carboxylic groups of the uronic acids and provide electrostatic binding between macromolecules. The hydrogels turn into aerogels with high surface area after dried under supercritical conditions (Valentin, Molvinger, Quignard, & Di Renzo, 2005). The resulting aerogels exhibit interesting properties, such as low mass density, continuous porosity, high surface area, and high electrical conductivity, as those of carbon aerogels (Kong, LeMay, Hulsey, Alviso, & Pekala, 1993; Pekala, Alviso, Kong, & Hulsey, 1992; Pekala, Alviso, & Lemay, 1992; Pekala, 1989). However, poor mechanical properties and high hydrophilicity have limited further development of alginate-based aerogels.

For the past several years, effort has been made to improve mechanical strength and toughness of aerogels. The attempted techniques include adding fiber in gel network to reinforce silica or carbon aerogels (Yang, Li, Luo, Yan, & Wang, 2011; Yang, Sun, Shi, & Liu, 2011), and incorporating inorganic clay (Pojanavaraphan & Magaraphan, 2008) into matrix. The nanocomposite polymer hydrogels represent gel systems with enhanced mechanical properties and thus display extremely high tensile strength and compression modulus before dried (Haraguchi, 2007; Schexnailder & Schmidt, 2009). However, there is less effort to reinforce alginate aerogel, which appeared later than traditional aerogels such as silica or carbon aerogel.

N,N′-methylenebisacrylamide can react with vinyl groups, hydroxyl compounds and amines and be used as a cross-linking agent during the formation of polymers such as polyacrylamide gel (Wu & Freeman, 2009; Yiamsawas, Kangwansupamonkon, Chailapakul, & Kiatkamjornwong, 2007). Carboxymethylcellulose is a cellulose derivative with carboxymethyl groups ($-CH_2-COOH$) bound to some of the hydroxyl groups of the glucopyranose

* Corresponding author. Tel.: +86 0898 66290799; fax: +86 0898 66279219.
E-mail address: lulingbin@126.com (L. Lu).

0144-8617/$ – see front matter
doi:10.1016/j.carbpol.2012.01.075

monomers that make up the cellulose backbone. Due to high molecular weight and long molecular chain-length, cellulose can act as a non-toxic reinforcing agent in polymers and composites (Cheng, Wang, & Rials, 2009; Zhou, Wu, Yue, & Zhang, 2011). The cold plasma technique is regarded as an effective method to modify hydrophobicity of polymeric surface (Pinto et al., 2010; Zou et al., 2011). According to previous research, it is also a good surface modification method for silica and carbon aerogels (Fang & Binder, 2007; Kim et al., 2000).

To further expand the potential application of alginate aerogels, in the current work we aim at the preparation of homogeneous, low density, low shrinkage and high strength as well as hydrophobic alginate-based aerogel. In this paper, the modified alginate-based aerogels were reported. As reinforcing agents, the influences of MBA and CMC were discussed. The plasma surface modification of alginate-based aerogel was also explored preliminarily.

2. Experimental

2.1. Materials

Sodium alginate (SA), carboxymethylcellulose (CMC, M_w = 160,000, 300–600 mPa s) were purchased from Tianjin Fuchen Chemical Reagents Factory. Calcium carbonate ($CaCO_3$), N,N′-methylenebisacrylamide (MBA), carbon tetrachloride (CCl_4), D-glucono-δ-lactone (GDL) was purchased from Tianjin Hongyan Chemical Reagents Factory, Tianjin Beilian Fine Chemicals Co., Ltd., Guangzhou Xilong Chemical Co., Ltd., and Shanghai Green Food Additive Co., Ltd., respectively. All chemical reagents were of analytical grade and directly used unless otherwise mentioned.

2.2. Preparation of alginate hydrogel and aerogel

The $CaCO_3$–GDL cross-linking system (Kuo & Ma, 2001) was used here. Sodium alginate was dissolved in deionized water. $CaCO_3$ powder was added into SA solution, mixed and stirred for uniformity. Reinforcing agent (MBA or CMC) was then added into the uniform suspension and stirred vigorously. GDL powder was subsequently added to the suspension and stirred to initiate gelation. The suspension was finally transferred into a mold, stood for 20 h to obtain hydrogel. To obtain aerogel, the hydrogel was dried by a FreeZone Plus 2.5 L Cascade Console Freeze Dry System (LABCONCO Co.). Samples were labeled as SA aerogel (without reinforcing agent), SA–MBA aerogel (MBA as the reinforcing agent) and SA–CMC aerogel (CMC as the reinforcing agent), respectively. For all alginate hydrogels, the calcium content was described with the calcium ion to carboxyl molar ratio. The calcium ion to carboxyl molar ratio 0.18 was defined as the basic standard and recorded as 1X.

2.3. Hydrophobic modification with the cold plasma treatment

The used HD-1A plasma equipment is provided by Chinese Academy of Sciences. The plasma excitation uses glow discharge with a variable power (from 0 to 250 W), which is coupled to a reactor. The incident power (Pi) and the reflected power (Pr) are measured with a power meter. The impedance is adjusted until the reflected power is very low (Pr < 3 W). The pumping system is composed of two oil diffusion pumps. Alginate aerogels without further pretreatment were placed at the sample holder. When the vacuum degree reached the lowest point, CCl_4 was introduced to the reactor with the rate 0.9 mL min^{-1}. The discharge system was then started when the vacuum degree maintained to a constant value. The hydrophobic aerogels were obtained after discharging under specified power and time.

2.4. Characterization

2.4.1. Estimation of gelation rate

Gelation rate was characterized with gelation time at which the mixture no longer flowed when the mold was tilted at 70° angle.

2.4.2. Aerogel density assay

Brick aerogel was maintained in a desiccator with allochroic silicagel overnight and then weighed as m_0. Volume 'length × width × height' of the aerogel was measured by a digital caliper and recorded as V. An average value from three replicated measurements was recorded for each sample. The density (ρ) was calculated by:

$$\rho = \frac{m_0}{V} \tag{1}$$

2.4.3. Measure of volume shrinkage

To evaluate the deformation of the aerogel resulted from the freeze drying, the volume shrinkage was measured by the following equation.

$$\text{volume shrinkage}(\%) = \frac{V_0 - V}{V_0} \times 100\% \tag{2}$$

V_0 is the volume of brick hydrogel and V is the volume of brick aerogel obtained after the freeze drying. An average value from three replicated measurements was recorded for each sample.

2.4.4. Estimation of mechanical properties

Mechanical properties of aerogel were evaluated by compressive strength. Since the alginate-based aerogels are brittle, it is hard to perform tensile strength measurement. In the estimation of compressive strength, we adopted a direct compression method by putting a series of weights to evaluate the bearing capacity of the alginate-based aerogels. The compressive strength was recorded at the moment of a sudden collapse of aerogel's structure. Compressive strength was obtained by the relationship:

$$\text{compressive strength} = \frac{F}{S} \tag{3}$$

where F is the bearing weight recorded when the structure of aerogel collapsed initially and S is the area of contact. An average value from three replicated measurements was recorded for each sample.

2.4.5. Measurement of contact angle

Water contact angles (drop, volume 10 μL) were performed using a HARKE Contact Angle Meter with a color CCD camera (20× objective). The contact angles were calculated according to the acquired photos with a direct angle measurement on its own software (HARK-SOFT).

2.4.6. Estimation of water and oil adsorption

Brick aerogel was weighed as m_0, and then immersed into distilled water or various oils at room temperature. After the equilibrium adsorption of water or oil, the aerogel was wiped with filter paper and weighed as m_1. An average value from three replicated measurements was recorded for each sample. The absorbency was calculated as follows:

$$\text{absorbency}(g\,g^{-1}) = \frac{m_1 - m_0}{m_0}. \tag{4}$$

2.4.7. Estimation of structure and morphology

The chemical structure of aerogel was investigated and compared with that of natural sodium alginate by Bruker FTIR spectrometer (model: TENSOR 27) with a resolution of 1 cm^{-1}.

Scanning electron microscopy (SEM) images of aerogel were obtained using a Hitachi S-3000N electron microscope after gold metallization.

3. Results and discussion

3.1. Preparation and physical properties of aerogels

For alginate hydrogel, calcium chloride is usually used as a source of calcium ions to initiate gelation. However, the gelation rate is too quick to control in the process, which leads the resulting hydrogel to nonuniformity and weak mechanical strength. At the same time, the complex-shaped three-dimensional structure is difficult to achieve (Skjåk-Bræk, Grasdalen, & Smidsrod, 1989). The $CaCO_3$–GDL binary system could make the gelation process slow and gave homogeneous structure to alginate hydrogel.

The gelation rate of gel system was carefully studied when reinforcing agents were introduced. These hydrogels exhibited an increasing gelation rate with the increase of SA concentration (as shown in Table S1). The pH value of the SA solution decreased from 6.44 to 6.16 with SA concentration increased from 1.5 to 3.5 wt%. The decrease of pH obviously accelerated the release of calcium, and therefore increased the gelation rate. The addding of MBA had little effct on gelation rate. The gelation time that SA–MBA system spent was almost the same to that in the SA system. However, the adding of CMC could decrease gelation rate effectively. The SA–CMC system spent more time on gelation, it might result from the increasing solution viscosity when more CMC dissolved in high SA concentration solution. Therefore, the slower rearrangement of polymer chains was caused and the effective crosslinks were relatively slowly formed.

A key observation was that density of alginate-based aerogels was low to 0.023 g cm^{-3} and increased with increasing SA concentration (as shown in Table S1). The reinforcing agent MBA did not show any evident influence on the density, while the CMC significantly increased density. It might be as a result of the high molecular weight of CMC. The trends of density indicated that SA concentration was important for the crosslinking formation. Higher SA concentration likely provides more crosslinking points and thereby leads to higher density with more effective crosslinks between alginate molecules and calcium ions.

The density of alginate-based aerogels was in the range of 0.039–0.067 g cm^{-3} with increasing of Ca^{2+} content (as shown in Table S2). The increase of Ca^{2+} content enhanced the inter- and intra-molecular interactions between alginate molecules, shortened the average distance of ionic crosslink, and resulted in the larger density.

To keep a good status, aerogel should have lower volume shrinkage. Comparable shrink profiles of these aerogels indicated that SA concentration and Ca^{2+} content affected volume shrinkage of aerogels less significantly, as well as reinforcing agents (shown in Tables S1 and S2). The resulting volume shrinkage maintained in the reasonable range of 15–30%.

The results of density and volume shrinkage suggested that the freeze-drying technology could be used as a convenient method to prepare alginate-based aerogel with low density and acceptable volume shrinkage. Considering appropriate gelation rate, low density and low volume shrinkage, the following experiments were processed with the samples made from 2 wt% SA solution, 1.5X Ca^{2+} content and 0.062 wt% MBA/0.76 wt% CMC unless otherwise mentioned. Fig. S1 represented the morphology images of the freeze-dried aerogels with low shrink and structural homogeneity.

3.2. Mechanical properties of alginate-based aerogels

Favorable mechanical properties are very important to brittle polysaccharide aerogel. Therefore, reinforcement of mechanical properties is the principal goal in our research on the alginate-based aerogel. Compressive strength, which led the structure of aerogel to collapse initially by bearing weight, increased slowly with SA concentration (Fig. 1). The compressive strength of reinforced aerogels was obviously superior to the aerogel without reinforcing agents. It was indicated that the reinforcing agents involved in the structure of aerogels and enhanced the interactive strength among molecules effectively. Because of strong polar groups, the interactive strength between CMC and SA molecules was enhanced with the increase of SA molecules. The stronger interactive strength made the compressive strength of SA–CMC aerogel increased dramatically when SA concentration was up to 3 wt%, as shown in Fig. 1. Improvement of

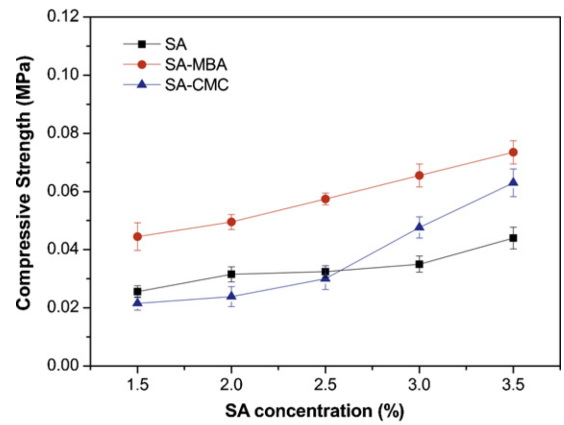

Fig. 1. Effect of SA concentration on compressive strength of aerogels.

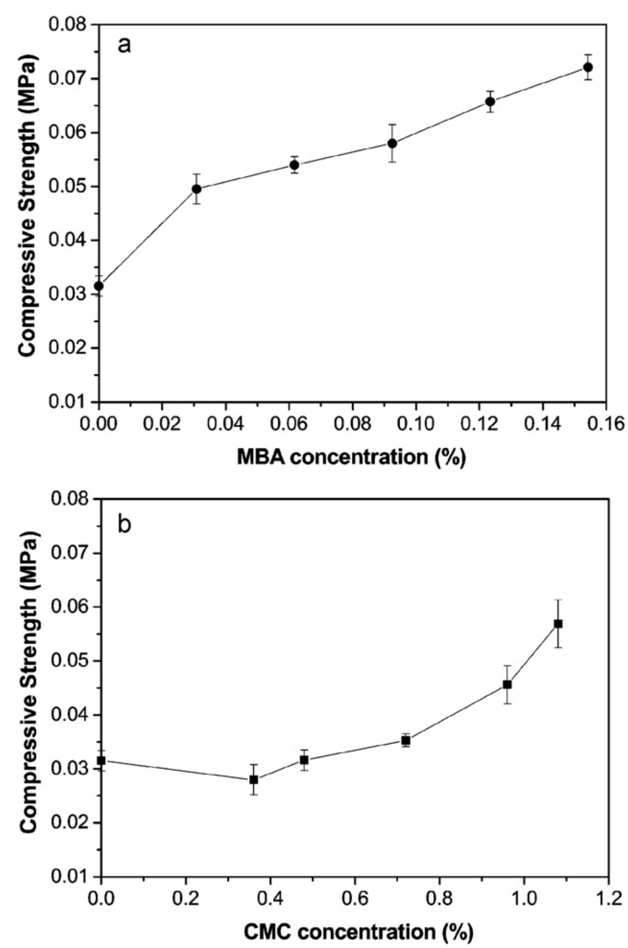

Fig. 2. Effect of reinforcing agents MBA (a) and CMC (b) concentration on compressive strength of aerogel.

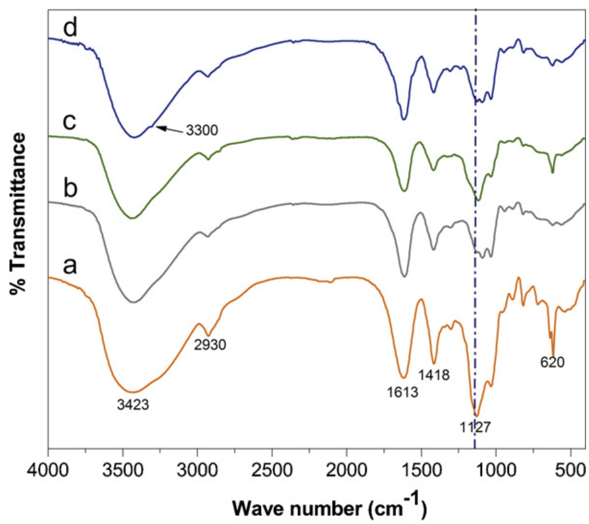

Fig. 3. FTIR spectra of natural SA (a), SA aerogel (b), SA–CMC aerogel (c) and SA–MBA aerogel (d).

compressive strength was also attributed to the increase of alginate molecular density, crosslinking density and entanglement.

Further observation on the influence of different reinforcing agents on the compressive strength of these aerogels was shown in Fig. 2. Compressive strength increased with the increase of MBA concentration, presumably due to increased H bonds. For SA–CMC aerogel, the increased viscosity with the increase of CMC concentration resulted in slower gelation rate. Hence, there was more time provided to process an even dispersion of $CaCO_3$ particles throughout the suspension before gelation completed.

According to their molecular structures, the presence of reinforcing agents was traced by FTIR spectra of the aerogels. In alginate molecule, there are many strong polar hydroxyl groups that are easy to form hydrogen bond with another electron donating groups, such as $-NH_2$, $-OH$ and C—O—C. The FTIR spectrum of natural SA showed a broad band assigned to hydroxyl groups at 3423 cm^{-1}, and C—O stretching vibration absorption peak at 1127 cm^{-1} [as shown in Fig. 3(a)]. Compared with the SA aerogel [Fig. 3(b)], the SA–MBA aerogel appeared a weak stretching vibration absorption peak of $-NH_2$ at 3300 cm^{-1}, which was almost covered by the broad hydroxyl groups absorption peak [as shown in Fig. 3(d)]. Because CMC and SA were basically similar in molecular structure, the SA–CMC aerogel and SA aerogel had the similar FTIR spectra. It was hard to tell the characteristic absorption peaks of CMC from Fig. 3(c). Compared with natural SA, the C—O stretching vibration absorption peaks of aerogels shifted to lower frequencies and the intensity of C—H flexural vibration absorption of aerogel significantly decreased at 620 cm^{-1}. These phenomena demonstrated the existent of H bond, which resulted from the generated 'egg box' model in calcium alginate gels (Braccini & Pérez, 2001). Therefore, it was concluded that the reinforcing agents mostly interacted with SA molecules through H bond in aerogels and reinforced aerogel's strength effectively.

The SEM images demonstrated the distinction of these aerogels. The SA aerogel presented irregular topography that suggested the lower strength [as shown in Fig. 4(a)]. Interestingly, the MBA–SA aerogel showed numerous unexpected nano-fibers formations [Fig. 4(b)], which speculated as the product of MBA self-polymerization. These nano-fibers were fixed as pillars in the aerogel's holes and supported the structure. Therefore, the SA–MBA aerogel appeared surprisingly higher strength. The SA–CMC aerogel showed relatively smooth surface [Fig. 4(c)], which also worked as an available supporter to the aerogel and provided superior mechanical properties. Considering the good film-forming characteristic of CMC, it was reasonable. The SEM images indicated that the reinforcing agents changed the microstructure and played a critical role to improve the aerogel's strength.

3.3. Hydrophobic modification of aerogel

The hydrophobic modification of aerogel consisted of a simple chlorination through CCl_4 plasma treatment. It was deduced that CCl_4 gas was dissociated by electronic impact under the electrical discharge as CF_4 dissociation (Bretagne, Epaillard, & Ricard, 1992; Fresnais, Chapel, & Poncin-Epaillard, 2006; Poncin-Epaillard et al., 1998).

$$e + CCl_4 \rightarrow 2e + CCl_3{}^{+} + Cl$$

$$e + CCl_4 \rightarrow e + CCl_3 + Cl$$

$$e + CCl_4 \rightarrow e + CCl_2 + 2Cl$$

$$e + CCl_4 \rightarrow e + CCl + 3Cl$$

CCl_x radicals acted as functionalization agent, and chlorine atom played as etching agent. The dissociation conditions were observed when discharge duration and power are taken as the control parameters (Fresnais et al., 2006).

For 3 min duration of the plasma treatment, the water contact angle of the SA aerogel was increasing from 0° to 49°, then this increase was followed by a plateau around 105–120° with discharge duration between 10 and 20 min (Fig. 5). For longer duration (30 min), this increase was not obvious any more. It was an indication that hydrophobic modification for alginate-based aerogels was successfully completed within 20 min. The highest value 129° of the contact angle was reached by the SA–MBA aerogel in 20 min. While at the same time, the highest contact angle of the SA–CMC aerogel was up to 120°, which was still higher than the 108° of the SA aerogel.

For the aerogels discharged with varying power, the contact angle was increasing to 135° with discharge power from 0 to 60 W (Fig. 6). However, under drastic conditions (discharge power higher than 60 W), the values of contact angle decreased significantly, this might be a result of degradation of alginate at harsh discharge power. Thus, high values of contact angle of aerogels should achieve under a mild discharge power less than 60 W.

By means of the CCl_4 plasma treatment, hydrophobic modification of reinforced aerogels achieved successfully. The variations of contact angle should correspond to different stages of competitive reactions between reinforced aerogels and CCl_4, such as cleaning, degradation and functionalization on aerogels' surface. The hydrophobic modification was successful in contrast to extremely hydrophilic unmodified alginate-based aerogels. The water drop could stand on the surface of the modified SA–MBA aerogel, as shown in Fig. S2(a). However, the water drop permeated the surface and distorted after 9 min as shown in Fig. S2(b). The reason was attributed to the porous structure and active chemical properties of modified aerogels. Therefore, our future work will be focused on the mechanism of the CCl_4 plasma treatment to alginate-based aerogel and further improvement of hydrophobicity.

3.4. Absorbability of modified aerogels

Nature property of the alginate-based aerogel was converted from hydrophilicity into hydrophobicity by the plasma treatment. Such a conversion, of course, would result in a change of application field. Comparisons of the water and oil absorbency between unmodified and modified aerogels were shown in Tables 1 and 2. It

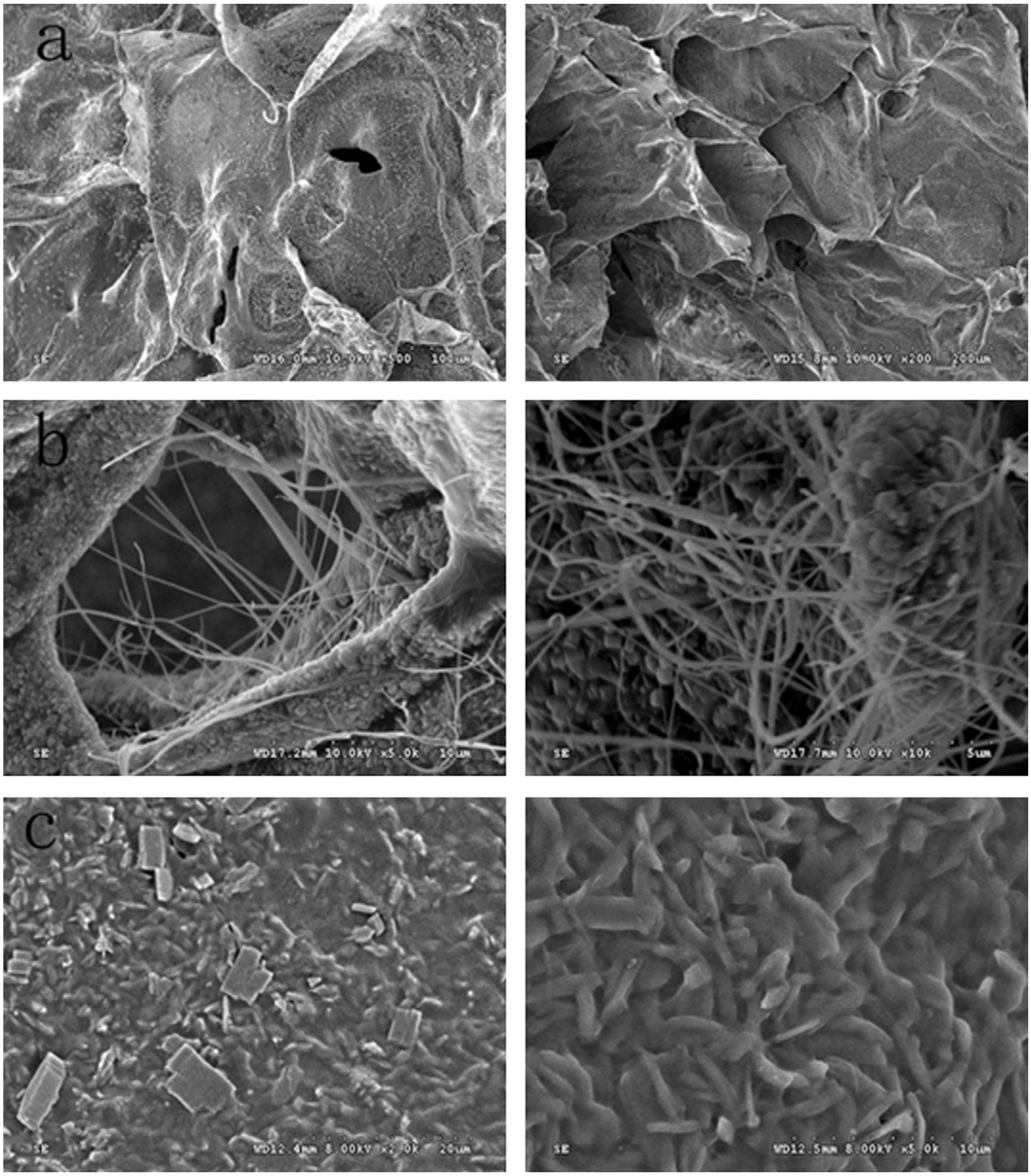

Fig. 4. SEM images of SA aerogel(a), SA–MBA aerogel (b) and SA–CMC aerogel (c).

Table 1
Water and oil absorbency of the unmodified alginate-based aerogels.

Sample	Absorbency ($g\,g^{-1}$)				
	Water	Peanut oil	Methyl silicone oil	Vacuum pump oil	Liquid paraffin
SA aerogel	29.2	2.54	1.66	2.74	2.27
SA–MBA aerogel	40.1	3.11	2.36	3.02	3.48
SA–CMC aerogel	36.5	2.84	2.2	3.7	3.95

Table 2
Oil absorbency of the modified hydrophobic alginate-based aerogels.

Sample	Absorbency ($g\,g^{-1}$)			
	Peanut oil	Methyl silicone oil	Vacuum pump oil	Liquid paraffin
SA aerogel	11.35	8.38	10.44	7.43
SA–MBA aerogel	13.25	11.17	12.04	10.20
SA–CMC aerogel	13.98	10.98	12.14	13.02

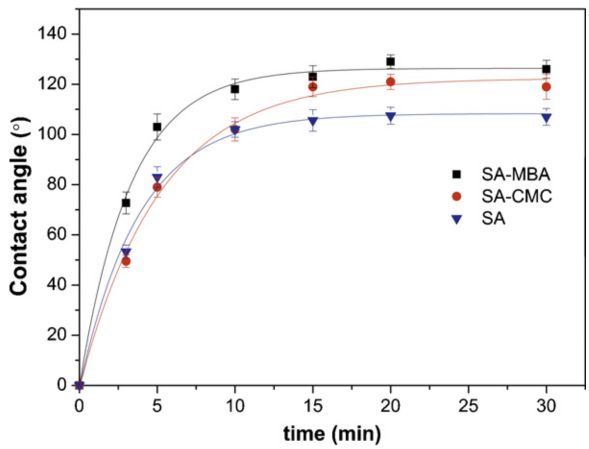

Fig. 5. Contact angle of aerogels treated by the CCl_4 plasma at 50 W versus discharge duration.

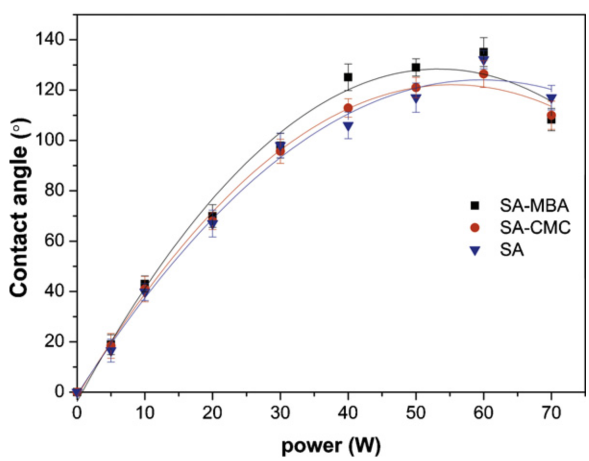

Fig. 6. Contact angle of aerogels treated by the CCl_4 plasma for 12 min versus discharge power.

was concluded from Table 1 that the hydrophilic aerogels were at an advantage in water absorption against oil absorption. Significantly, the modified hydrophobic aerogels exhibited high oil absorbency as shown in Table 2. Such a value of oil absorbency was consistent with high oil-absorptive polymers such as butyl methacrylate–lauryl methacrylate copolymeric fibers (kerosene absorbency, 8 g g^{-1}) (Feng & Xiao, 2006) and oil gels based on EPDM/4-tert-butylstyrene (kerosene absorbency, 6–23 g g^{-1}) (Wu & Zhou, 2009). Therefore, the hydrophobic alginate-based aerogels showed a potential application in oil absorption fields.

4. Conclusions

Homogeneous low-density alginate-based aerogel was successfully prepared by ionotropic gelation of sodium alginate with $CaCO_3$–GDL binary system as the crosslink agent and the freeze-drying technology. Slower gelation rate was advantageous to aerogel homogeneity which can be achieved by control SA concentration and Ca^{2+} content. The obtained aerogels showed low density and low volume shrinkage. This work implies that the freeze-drying technology can be used as a convenience method to obtain low-density alginate-based aerogels. In order to reinforce the mechanical strength of alginate-based aerogel, N,N′-methylenebisacrylamide and carboxymethylcellulose were introduced into the alginate hydrogel matrix as reinforcing agents, respectively. The reinforcing agents had strong interaction with alginate matrix through hydrogen bond. The compressive strength of reinforced aerogels was higher than that of the pure alginate aerogel. Meanwhile, these aerogels still retained low density and low volume shrinkage. The surface modification of alginate aerogel was achieved successfully by the CCl_4 plasma treatment. The highly hydrophobic alginate-based aerogels were obtained under mild plasma conditions. It offers us a good method to modify the surface properties of polysaccharide aerogels. The study on adsorption behavior suggested the hydrophobic alginate-based aerogels can be used as oil-absorptive materials. This work provides a novel idea for expanding the application field of alginate-based aerogel. Future work will be focused on further improvement of strength and hydrophobicity of alginate-based aerogels, and a better knowledge of the mechanism of plasma hydrophobic modification.

Acknowledgment

This work was supported by the Important Science & Technology Specific Projects of Hainan Province (No. ZDZX20100009).

Appendix A. Supplementary data

Supplementary data associated with this article can be found, in the online version, at doi:10.1016/j.carbpol.2012.01.075.

References

Augst, A. D., Kong, H. J., & Mooney, D. J. (2006). Alginate hydrogels as biomaterials. *Macromolecular Bioscience*, *6*, 623–633.
Božanić, D. K., Trandafilović, L. V., Luyt, A. S., & Djoković, V. (2010). 'Green' synthesis and optical properties of silver–chitosan complexes and nanocomposites. *Reactive and Functional Polymers*, *70*, 869–873.
Braccini, I., & Pérez, S. (2001). Molecular basis of Ca^{2+}-induced gelation in alginates and pectins: The egg-box model revisited. *Biomacromolecules*, *2*, 1089–1096.
Bretagne, J., Epaillard, F., & Ricard, A. (1992). Excited states of CF_4 plasma for polymerization of TMPTA monomer. *Journal of Polymer Science Part A: Polymer Chemistry*, *30*, 323–328.
Chan, A. W., Whitney, R. A., & Neufeld, R. J. (2009). Semisynthesis of a controlled stimuli-responsive alginate hydrogel. *Biomacromolecules*, *10*, 609–616.
Cheng, Q., Wang, S., & Rials, T. G. (2009). Poly(vinyl alcohol) nanocomposites reinforced with cellulose fibrils isolated by high intensity ultrasonication. *Composites Part A: Applied Science and Manufacturing*, *40*, 218–224.
Chung, T. W., Yang, J., Akaike, T., Cho, K. Y., Nah, J. W., Kim, S. I., & Cho, C. S. (2002). Preparation of alginate/galactosylated chitosan scaffold for hepatocyte attachment. *Biomaterials*, *23*, 2827–2834.
Dang, J. M., & Leong, W. K. (2006). Natural polymers for gene delivery and tissue engineering. *Advanced Drug Delivery Reviews*, *58*, 487–499.
Dar, A., Shachar, M., Leor, J., & Cohen, S. (2002). Optimization of cardiac cell seeding and distribution in 3D porous alginate scaffolds. *Biotechnology and Bioengineering*, *80*, 305–312.
Donati, I., Holtan, S., Mørch, Y. A., Borgogna, M., Dentini, M., & Skjåk-Braek, G. (2005). New hypothesis on the role of alternating sequences in calcium–alginate gels. *Biomacromolecules*, *6*, 1031–1040.
Draget, K. I., Smidsrød, O., & Skjåk-Bræk, G. (2002). Alginates from algae. In E. J. Vandamme, S. De Baets, & A. Steinbüchel (Eds.), *Biopolymers polysaccharides from eukaryotes* (pp. 215–244). Weinheim: Wiley-VCH.
Fang, B., & Binder, L. (2007). Enhanced surface hydrophobisation for improved performance of carbon aerogel electrochemical capacitor. *Electrochimica Acta*, *52*, 6916–6921.
Feng, Y., & Xiao, C. F. (2006). Research on butyl methacrylate–lauryl methacrylate copolymeric fibers for oil absorbency. *Journal of Applied Polymer Science*, *101*, 1248–1251.
Fresnais, J., Chapel, J. P., & Poncin-Epaillard, F. (2006). Synthesis of transparent superhydrophobic polyethylene surfaces. *Surface and Coatings Technology*, *200*, 5296–5305.
Haraguchi, K. (2007). Nanocomposite hydrogels. *Current Opinion in Solid State & Materials Science*, *11*, 47–54.
Hashimoto, T., Suzuki, Y., Tanihara, M., Kakimaru, Y., & Suzuki, K. (2004). Development of alginate wound dressings linked with hybrid peptides derived from laminin and elastin. *Biomaterials*, *25*, 1407–1414.
Kim, J. J., Park, H. H., & Hyun, S. H. (2000). The effects of plasma treatment on SiO_2 aerogel film using various reactive (O_2, H_2, N_2) and non-reactive (He, Ar) gases. *Thin Solid Films*, *377–378*, 525–529.
Kong, F. M., LeMay, J. D., Hulsey, S. S., Alviso, C. T., & Pekala, R. W. (1993). Gas permeability of carbon aerogels. *Journal of Materials Research*, *8*, 3100–3105.
Kuo, C. K., & Ma, P. X. (2001). Ionically crosslinked alginate hydrogels as scaffolds for tissue engineering: Part 1. Structure, gelation rate and mechanical properties. *Biomaterials*, *22*, 511–521.

Mierisch, C. M., Cohen, S. B., Jordan, L. C., Robertson, P. G., Balian, G., & Diduch, D. R. (2002). Transforming growth factor-β in calcium alginate beads for the treatment of articular cartilage defects in the rabbit. *Journal of Arthroscopic and Related Surgery*, *18*, 892–900.

Pekala, R. W. (1989). Organic aerogels from the polycondensation of resorcinol with formaldehyde. *Journal of Materials Science*, *24*, 3221–3227.

Pekala, R. W., Alviso, C. T., Kong, F. M., & Hulsey, S. S. (1992). Aerogels derived from multifunctional organic monomers. *Journal of Non-Crystalline Solids*, *145*, 90–98.

Pekala, R. W., Alviso, C. T., & Lemay, J. D. (1992). Organic aerogels: A new type of ultrastructured polymer. In L. L. Hench, & J. K. West (Eds.), *Chemical processing of advanced materials*. New York: Wiley-VCH (pp. 671–683)

Pinto, S., Alves, P., Matos, C. M., Santos, A. C., Rodrigues, L. R., Teixeira, J. A., & Gil, M. H. (2010). Poly(dimethyl siloxane) surface modification by low pressure plasma to improve its characteristics towards biomedical applications. *Colloids and Surfaces B: Biointerfaces*, *81*, 20–26.

Pojanavaraphan, T., & Magaraphan, R. (2008). Prevulcanized natural rubber latex/clay aerogel nanocomposites. *European Polymer Journal*, *44*, 1968–1977.

Poncin-Epaillard, F., Wang, W., Ausserré, D., Scharzenbach, W., Derouard, J., & Sadeghi, N. (1998). Surface modification of hexatriacontane by CF_4 plasmas studied by optical emission and threshold ionization mass spectrometries. *The European Physical Journal – Applied Physics*, *4*, 181–191.

Quignard, F., Valentin, R., & Di Renzo, F. (2008). Aerogel materials from marine polysaccharides. *New Journal of Chemistry*, *32*, 1300–1310.

Robitzer, M., David, L., Rochas, C., Di Renzo, F., & Quignard, F. (2008). Nanostructure of calcium alginate aerogels obtained from multistep solvent exchange route. *Langmuir*, *24*, 12547–12552.

Robitzer, M., Di Renzo, F., & Quignard, F. (2011). Natural materials with high surface area. Physisorption methods for the characterization of the texture and surface of polysaccharide aerogels. *Microporous and Mesoporous Materials*, *140*, 9–16.

Schexnailder, P., & Schmidt, G. (2009). Nanocomposite polymer hydrogels. *Colloid and Polymer Science*, *287*, 1–11.

Shapiro, L., & Cohen, S. (1997). Novel alginate sponges for cell culture and transplantation. *Biomaterials*, *18*, 583–590.

Skjåk-Bræk, G., Grasdalen, H., & Smidsrod, O. (1989). Inhomogeneous polysaccharide ionic gels. *Carbohydrate Polymers*, *10*, 31–54.

Valentin, R., Molvinger, K., Quignard, F., & Di Renzo, F. (2005). Methods to analyse the texture of alginate aerogel microspheres. *Macromolecular Symposium*, *222*, 93–102.

Wang, T., Liu, D., Lian, C., Zheng, S., Liu, X., Wang, C., & Tong, Z. (2011). Rapid cell sheet detachment from alginate semi-interpenetrating nanocomposite hydrogels of PNIPAm and hectorite clay. *Reactive and Functional Polymers*, *71*, 447–454.

Wu, B., & Zhou, M. H. (2009). Quantitative effects of synthesis conditions on oil absorptive properties of oil gels based on EPDM/4-tert-butylstyrene. *Journal of Applied Polymer Science*, *112*, 2213–2220.

Wu, Y. H., & Freeman, B. D. (2009). Structure, water sorption, and transport properties of crosslinked N-vinyl-2-pyrrolidone/N,N′-methylenebisacrylamide films. *Journal of Membrance Science*, *344*, 182–189.

Yang, J., Li, S., Luo, Y., Yan, L., & Wang, F. (2011). Compressive properties and fracture behavior of ceramic fiber-reinforced carbon aerogel under quasi-static and dynamic loading. *Carbon*, *49*, 1542–1549.

Yang, X., Sun, Y., Shi, D., & Liu, J. (2011). Experimental investigation on mechanical properties of a fiber-reinforced silica aerogel composite. *Materials Science and Engineering A*, *528*, 4830–4836.

Yiamsawas, D., Kangwansupamonkon, W., Chailapakul, O., & Kiatkamjornwong, S. (2007). Synthesis and swelling properties of poly[acrylamide-co-(crotonic acid)] superabsorbents. *Reactive and Functional Polymers*, *67*, 865–882.

Zhou, C., Wu, Q., Yue, Y., & Zhang, Q. (2011). Application of rod-shaped cellulose nanocrystals in polyacrylamide hydrogels. *Journal of Colloid and Interface Science*, *353*, 116–123.

Zou, L., Vidalis, I., Steele, D., Michelmore, A., Low, S. P., & Verberk, J. Q. J. C. (2011). Surface hydrophilic modification of RO membranes by plasma polymerization for low organic fouling. *Journal of Membrance Science*, *369*, 420–428.